Unique Cellulose/Polydimethylsiloxane Blends as Advanced Hybrid Material for Organic Solvent Nanofiltration and Pervaporation Membranes

Article *in* Journal of Materials Chemistry A · June 2018

DOI: 10.1039/C8TA02697A

CITATIONS
3

READS
187

4 authors, including:

Tiara Puspasari
King Abdullah University of Science and Technology
32 PUBLICATIONS **264** CITATIONS

SEE PROFILE

Giuseppe Genduso
King Abdullah University of Science and Technology
20 PUBLICATIONS **157** CITATIONS

SEE PROFILE

Journal of
Materials Chemistry A

Accepted Manuscript

This article can be cited before page numbers have been issued, to do this please use: T. Puspasari, T. Chakrabarty, G. Genduso and K. Peinemann, *J. Mater. Chem. A*, 2018, DOI: 10.1039/C8TA02697A.

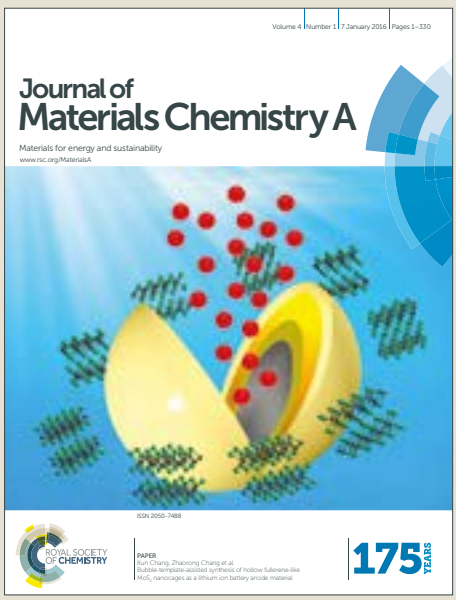

ROYAL SOCIETY OF CHEMISTRY

rsc.li/materials-a

View Article Online
DOI: 10.1039/C8TA02697A

Journal of Material Chemistry A

ARTICLE

Unique Cellulose/Polydimethylsiloxane Blends as Advanced Hybrid Material for Organic Solvent Nanofiltration and Pervaporation Membranes

Received 00th January 20xx,
Accepted 00th January 20xx

DOI: 10.1039/x0xx00000x

www.rsc.org/

Tiara Puspasari[a], Tina Chakrabarty[a], Giuseppe Genduso[b], Klaus-Viktor Peinemann[a]*

A novel method for the preparation of cellulose-polydimethylsiloxane (PDMS) blend membranes for organic solvent nanofiltration (OSN) and ethanol pervaporation is presented. The elegance of this approach lies on the use of trimethylsilyl cellulose (TMSC), a hydrophobic cellulose derivative, for the blend membrane fabrication followed by a simple hydrolysis to convert the TMSC back into cellulose. The use of TMSC does not only allow cellulose processing in the common organic solvents, but also enables the creation of highly compatible cellulose-PDMS blend membranes. The proper composition of the blend membrane gave the best OSN performance with more than 10 L/m^{2}hbar acetone permeance and around 750 Da molecular weight cut-off. The blend membrane can be used for OSN with any other solvents regardless their polarity. The same membrane also displayed an excellent pervaporation performance with a separation factor of 14 and a flux of 1.6 kg/m^{2}h flux using a 5 wt% ethanol water mixture at room temperature. The blending of PDMS with cellulose resulted in a 100% increase of the separation factor when compared with pure PDMS. This surprising performance is a consequence of the good miscibility of the blending polymers, which can be obtained through this unique pathway. Overall, this study demonstrates a simple, efficient, scalable and the only possible way reported to date to combine the superiority of cellulose and PDMS as a low-cost and stable membrane for solvent separation.

1 Introduction

Organic solvents are immensely important in an evolving range of industrial applications. The global solvent market reached US$25 billion in 2013 and is expected to increase by 4% per year until 2021[1]. Membrane technology is emerging as a viable process for molecular separation in various media including organic solvents. Compared to the conventional distillation process, membrane technology is attractive as it is cost-effective, generates smaller footprint, and can be operated in a much simpler way. It is projected to consume up to 90% less energy currently used for distillation[2].

In particular, organic solvent nanofiltration (OSN), which is also known as solvent resistant nanofiltration (SRNF), and pervaporation are developed for solvent separation and purification driven solely by a pressure gradient across the membrane. OSN is a relatively new yet promising membrane technology for the separation of molecules in the range of 200-1,000 Da[3]. Recent advances in OSN have led to various applications in the pharmaceutical[4, 5], petrochemical[6] and food industry[7]. The state-of-the-art OSN membranes are predominantly derived from polyimide in an integrally skinned asymmetric configuration[8]. In these membranes, the selective and support layer are formed simultaneously from the same material, creating limitation in the solvent fluxes[9]. Alternatively, OSN membranes can be fabricated as a thin film composite, allowing the optimization of the active layer independently from the support. Additionally, given that the typical OSN membranes can only be used for solvents with similar polarity[3], membranes that allow fast permeation of a wide range of solvents are highly desirable. Pervaporation is another membrane technology for the separation of mixtures containing organic solvents and water. It has been widely applied in various industrial processing including solvent dehydration, product recovery and waste water treatment[10, 11]. Pervaporation is very useful especially to treat mixtures that cannot be separated by the conventional distillation, such as azeotropes, mixtures of solvents with close boiling points or with temperature sensitivity[12]. The process combines the selective permeation and evaporation of certain component in the mixtures based on the solution-diffusion mechanism. The permeating components are first dissolved in the membrane on the feed side, diffuse across the membrane and finally desorb as vapors on the permeate side. The permeating vapors are immediately condensed to create the constant driving force, namely the partial vapor pressure gradient across the membrane. Pervaporation is a solubility-controlled mass transfer where the membrane

[a] Multicomponent Polymer-based Membranes Group, Advanced Membranes and Porous Material Research Center (AMPM), 4700 King Abdullah University of Science and Technology (KAUST), Thuwal 23955-6900, Kingdom of Saudi Arabia.
[b] Functional Polymer Membranes Group, AMPM.
Electronic Supplementary Information (ESI) available:. See DOI: 10.1039/x0xx00000x

View Article Online
DOI: 10.1039/C8TA02697A

affinity to the permeating component is crucial for a successful separation. Despite the significant progress made in both separations in the last decade, it is still challenging to fabricate high performance membranes from low-cost materials through simple processes.

Polydimethylsiloxane (PDMS), often referred to as "silicon rubber", has emerged as an important membrane material with extensive uses in gas and liquid separations. It is a highly flexible polymer with a very low glass transition temperature (around -125°C)[13, 14] attributed to the free rotation of the Si-O bonds, making it highly processable and very permeable to numerous molecules. PDMS turns into a macromolecular mesh when swollen with non-polar solvents like hexane, compromising its selectivity. Various techniques have been developed to improve the separation properties of PDMS. In particular, incorporation of hydrophilic segments such as polyethylene oxide[15, 16], polyethylene glycol[17], poly(methyl methacrylate)[18, 19], dopamine[20], and polyimide[21] into PDMS have shown various degrees of selectivity improvement in gas separation and pervaporation, attributed either to the microphase-separated structure or the increasing chain rigidity.

Cellulose is another attractive polymer for membrane manufacturing due to its abundant availability, low cost, environment benignancy, and fascinating physiochemical properties. In particular, cellulose possess a unique molecular architecture, at which the repeating β-D-glucopyranose molecules are covalently bound through acetal linkages (β-1,4-glucan), making it chemically resistant, inherently stiff and strongly hydrophilic. These properties endow cellulose as an excellent candidate for size exclusion carried out in solvent media, especially in polar solvents. However, its chemical stability also creates difficulties in fabricating cellulose membranes using the common organic solvents, advocating the use of the derivation-regeneration route as an alternative to the one-step fabrication using exotic or toxic solvents.

Intrigued by the remarkable properties of the aforementioned polymers while considering their limitations in the separation, we fabricated cellulose-PDMS membranes simply by physical blending. Compared to the complicated copolymerization approach commonly applied to modify PDMS, physical blending is more time- and cost-effective to modulate membrane performance by combining the superiority of the constituting polymers. Unfortunately, blending of these polymers was previously not possible due to their contrary properties. In the present study, blending of cellulose and PDMS is realized by first modifying cellulose into trimethylsilyl cellulose (TMSC), followed by the in situ regeneration of TMSC back into cellulose after the blend membrane fabrication. TMSC is an easily synthesized cellulose derivative that has been used earlier to create microporous membranes with remarkable performance in nanofiltration and water vapor/gas separation[22-25]. Mixtures of PDMS and TMSC can be dissolved in hexane without visible phase separation enabling the preparations of transparent films and coatings. The blends remains homogeneous even after cellulose regeneration. The fabricated membranes were investigated for molecular separation in organic solvents through organic solvent nanofiltration (OSN) and pervaporation. The combination of the rubbery PDMS and the rigid cellulose structure is expected to overcome the selectivity-permeability tradeoff in OSN, while the created amphiphilic feature is anticipated to improve the PDMS selectivity in ethanol-water pervaporation. Commercial polyacrylonitrile ultrafiltration membranes (GMT GmbH, Germany) were used as supports for the thin film coating. These membranes are stable in a wide range of solvents. The successful creation of the blend membranes was proved by infrared spectroscopy and elemental analysis. The changes of the membrane properties upon the cellulose regeneration were also investigated.

Table 1 Composition of the membranes prepared in this study.

Membrane	TMSC (wt%)	PDMS (wt%)	Crosslinking	VPH
RC	2	-	-	15 min
75RC	1.5	0.5	100°C, 2h	15 min
50RC	1	1	100°C, 2h	15 min
25RC	0.5	1.5	100°C, 2h	15 min
PDMS2	-	2	100°C, 2h	-
PDMS4	-	4	100°C, 2h	-
PDMS6	-	6	100°C, 2h	-

2 Experimental Section

2.1 Materials

TMSC was prepared from microcrystalline cellulose (Avicel

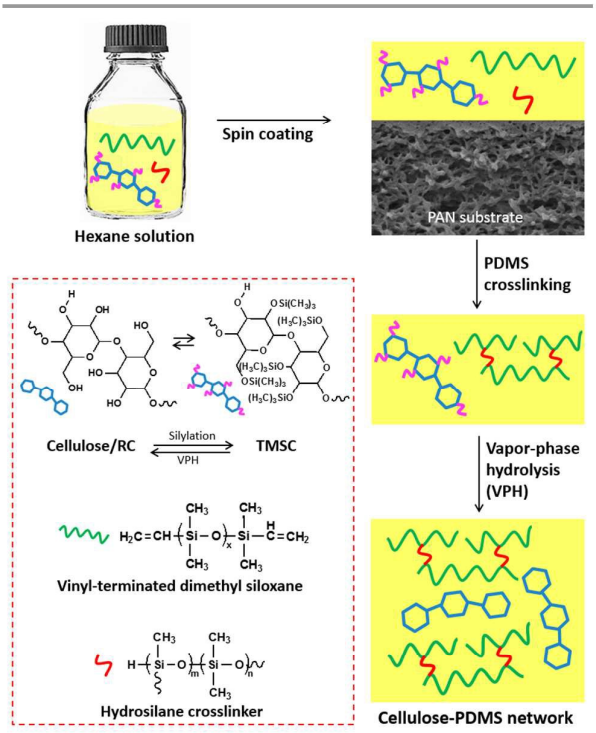

Scheme 1 Preparation of cellulose-PDMS blend composite membranes on a PAN support.

View Article Online
DOI: 10.1039/C8TA02697A

PH101, Fluka) and was characterized according to our previous work[24, 25]. Dimethylacetamide (DMAc), lithium chloride, hydrochloric acid (HCl), *n*-hexane, methanol, acetone, tetrahydrofuran, ethanol, acetonitrile, chloroform, and toluene were purchased from Sigma Aldrich and used without further purification. Isopropanol was purchased from Acros Organics. MilliQ water was used in the pervaporation experiments. PDMS pre-mixed kit consisting of Sylgard 184A as a pre-polymer and Sylgard 184B as a crosslinker was obtained from Sewang Hitech Co. Ltd. (South Korea). Commercial polyacrylonitrile (GMT GmbH, Germany) ultrafiltration membranes were used as supports. Dyes and polystyrene with different molecular weights for OSN experiments were purchased from Sigma Aldrich.

2.2 Membrane Preparation

Coating solutions were prepared by dissolving TMSC, PDMS or mixture of both in n-hexane at room temperature. The composition of each membrane is listed in Table 1. A 10:1 ratio of pre-polymer to the crosslinker was used for PDMS formation, following the recommendation from the manufacturer. Polymer deposition on the PAN support was carried out by spin coating at a 4,000 rpm and 500 $rpms^{-1}$ speed and acceleration, respectively. TMSC-coated membranes were transformed back into cellulose through a vapor-phase hydrolysis (VPH) using a 10% HCl solution for 15 minutes (Figure S3), whereas pure PDMS membranes underwent curing at 100°C for 2h. In the case of the blend membranes, the coated supports experienced both curing and hydrolysis consecutively as illustrated in Scheme 1.

2.3 Membrane Characterization

The ATR-IR spectra of the membranes were collected using a Fischer Scientific Nicolet iS10 spectrometer and were recorded in the range between 500 and 4,000 cm^{-1} over 16 scans. The bare PAN support was measured as a background. The XPS experiments were performed on a Kratos Axis Ultra DLD instrument equipped with a monochromatic Al Kα x-ray source (hv = 1486.6 eV) operated at a power of 150 W and under UHV conditions in the range of 10–9 mbar. All spectra were recorded in hybrid mode using electrostatic and magnetic lenses and an aperture slot of 300 µm × 700 µm. The survey and high-resolution spectra were acquired at fixed analyzer pass energies of 160 eV and 20 eV, respectively. The samples were mounted in floating mode in order to avoid differential charging and XPS spectra were therefore acquired using charge neutralization. A Lorentzian-Gaussian function was used for the curve fitting on the C1s, Si2p and O1s region at their corresponding binding energies. Energy-dispersive X-ray (EDX) spectroscopy analysis was performed using an OXFORD EDX equipped with X-MaxN detector, an 80 mm^2 SDD sensor and AZtecEnergy analysis software. The accelerating voltage was 10 keV with a probe current of 5.5 nA. The membrane hydrophilicity was determined by a static water contact angle (WCA) measurement using a Krüss drop shape analyzer—DSA100 with monochrome interline CCD camera. Surface and cross-section SEM imaging was performed on the 3 nm iridium-coated membranes using a Teneo scanning electron microscopy at 3 kV with a working distance between 3-5 mm. The samples for cross-section imaging were fractured in liquid nitrogen. The surface topographies were analyzed by an atomic force microscopy (AFM) on an ICON Veeco microscope operating in the tapping mode using commercial silicon TM AFM tips (MPP 12100).

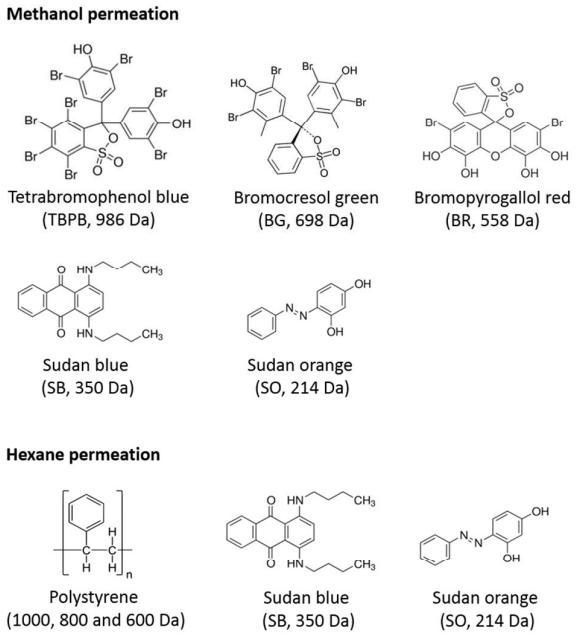

Figure 1 Neutral markers used in the OSN experiments.

2.4 OSN Experiment

All nanofiltration experiments were carried out using a commercial HP4750 dead-end filtration cell (Sterlitech Corporation, USA) with an effective area of 13.85 cm^2 pressurized by nitrogen. Rejection experiments were carried out using either methanol or hexane containing neutral polystyrene and or neutrally charged dyes as markers. Permeances of the pure solvents were tested using methanol, hexane, ethanol, isopropanol, tetrahydrofuran (THF), toluene, chloroform, acetone, and acetonitrile. Prior to the measurements, the membranes were soaked in the respecting solvents for minimum 24 hours to reach equilibrium. The permeance, J_w (L/m^2hbar), which is the pressure-normalized flux, was calculated using eq. (1),

$$J_w = \frac{V}{A \times \Delta t \times P} \quad (1)$$

where V is the volume of the permeate (L), A is the active membrane area (m^2), Δt is the time for permeate collection (h), and P is the trans–membrane pressure (bar). Rejection value was determined as a ratio of permeate concentration over the averaged concentration of the initial and final feed solution following eq. (2). The rejection of dyes and

View Article Online
DOI: 10.1039/C8TA02697A

polystyrene was monitored using a NanoDrop 2000/2000c spectrophotometer (Thermo Fisher Scientific).

$$\text{Rejection (\%)} = \left(1 - \frac{C_p}{C_f}\right) \times 100 \qquad (2)$$

2.5 Pervaporation Experiment

Figure S1 and S2 show the in-house designed pervaporation unit. It is known that under turbulent flow it is possible to maximize feed side diffusion rate minimizing any polarization phenomena. Hence, a dead end cell that allows mixing directly on top of the membrane was used, setting high stirring rates (>400 rpm). The dead-end cell was modified for pervaporation, allowing sampling retentates and sensing temperatures directly at the stirring zone (i.e., just above the membrane). The membrane active-area was 11.33 cm^2. A Honeywell™ Super TJE of 14 PSIa pressure transducer was used to sense permeate pressure. Both temperature and transducer signals were recorded via a computer interface based on LABVIEW®. Two vacuum traps immersed in liquid nitrogen allowed collecting permeates. The combination of unit-configuration, pump installed, and membranes used permitted permeate-pressures even lower than 20 mATM.

The composition of the collected permeate was determined using an Agilent gas chromatography model 7890A with a flame ionization detector and DB-WAX column (30 m × 320µm × 0.25µm J & W 123-7032, 250°C). The total flux J_p (kg/m^2h), was calculated according to eq. (3) by dividing the weight of the collected sample, m (kg), with the effective membrane area, A (m^2), and time difference, Δt (h). The separation factor (SF), which is the basic parameter to measure the pervaporation performance, was calculated according to eq. (4), where X and Y are the weight fraction of species in the permeate and feed, respectively. Subscript a and b denote ethanol and water, respectively.

$$J_p = \frac{m}{A \times \Delta t} \qquad (3)$$

$$\text{SF} = \frac{\left(\frac{Xa}{Xb}\right)_p}{\left(\frac{Ya}{Yb}\right)_F} = \frac{\frac{(Xa)_p}{(1-Xa)_p}}{\frac{(Ya)_F}{(1-Ya)_F}} \qquad (4)$$

The pervaporation experiments were carried out using aqueous feed solutions containing 5 wt% and 10 wt% ethanol at 24°C and 60°C under atmospheric feed pressure and vacuum downstream.

3 Results and Discussion

3.1 The Changes of the Membrane Properties Before and After Vapor-Phase Hydrolysis

As illustrated in Scheme 1, the membrane preparation protocol involves 3 consecutive steps: the modification of cellulose into TMSC to create a well-miscible polymer blend for solution coating, followed by PDMS curing and eventually an acid-vapor hydrolysis (VPH) to transform the TMSC back to cellulose. As a polymer with Si-O bonds, TMSC bears similar chemical properties to PDMS, enabling the preparation of a highly compatible polymer mixture in the commonly used solvents like *n*-hexane. PDMS formation was performed through the catalytic hydrosilylation between the vinyl-terminated dimethylsiloxane and the hydrosilane-containing crosslinker (see Scheme 1). Curing at 100°C for 2 hours was performed to complete the reaction. TMSC in the blend membrane was then regenerated back to cellulose through a vapor-phase hydrolysis (VPH) using hydrochloric acid. This step was necessary for TMSC to regain the cellulose structure, yet it could be detrimental for PDMS as it can lead to depolymerization. Because of the higher reactivity the acid vapor attacked preferentially the silyl group in TMSC rather than the siloxane positioned in the PDMS backbone. As described in our earlier work[25] a 15 min vapor hydrolysis was required to completely remove the silyl groups and restore the hydroxyl groups previously present in cellulose. To elucidate the TMSC transformation in the blend membrane, we recorded FTIR spectra of the 50RC membrane before and after vapor hydrolysis. From Figure 2A it is apparent that upon hydrolysis a strong O-H peak appeared between 3,000-3,700 cm^{-1} accompanied by the strong decrease of the TMS-related peaks around 1,250 and 840 cm^{-1}, indicating that a significant amount of TMS has been cleaved. These results were concomitant with the atomic composition obtained from XPS measurement (Figure 2B), where the silicon percentage decreased by more than half upon cellulose

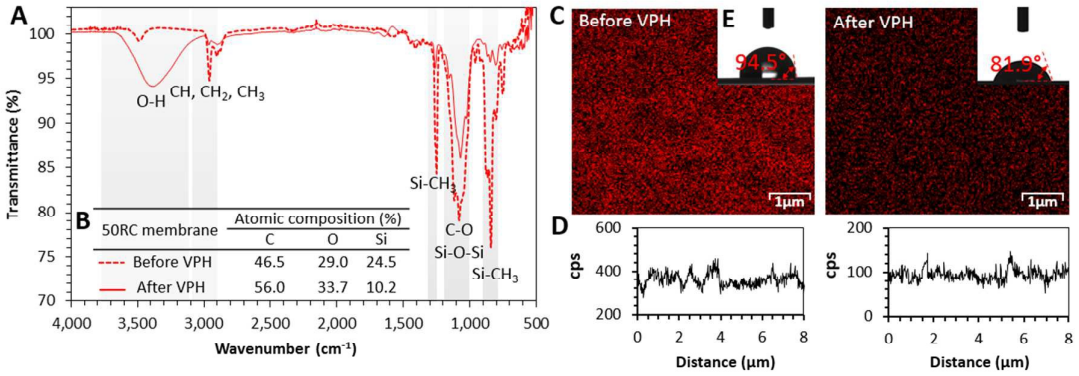

Figure 2 The changes of the 50RC properties before and after vapor-phase hydrolysis (VPH). **A.** ATR-IR spectra using the bare PAN support as a background, **B.** XPS survey

View Article Online
DOI: 10.1039/C8TA02697A

regeneration.

The blend membranes also demonstrated a good homogeneity, as seen in the large-scale silicon map recorded using EDX spectroscopy (Figure 2C). The silicone-related compounds were represented as red dots. EDX line scan image presented in Figure 2D shows that the silicone content of the membrane before VPH was significantly higher than after the reaction, supporting the aforementioned ATR-IR and XPS results. These chemistry changes were also followed by the decrease in the surface water contact angle (Figure 2E), realized from the substitution of the hydrophobic siloxane groups by the hydrophilic hydroxyls.

3.2 Final Membrane Structure and Morphology

Different compositions of TMSC and PDMS in the blend membranes were prepared and their final structure and morphology were characterized. The ATR-IR spectra of the pure and blend membranes are presented in Figure 3A. Among the most intense peaks associated with PDMS were Si-CH_3 bands at about 1,260 and 795 cm^{-1} as well as the

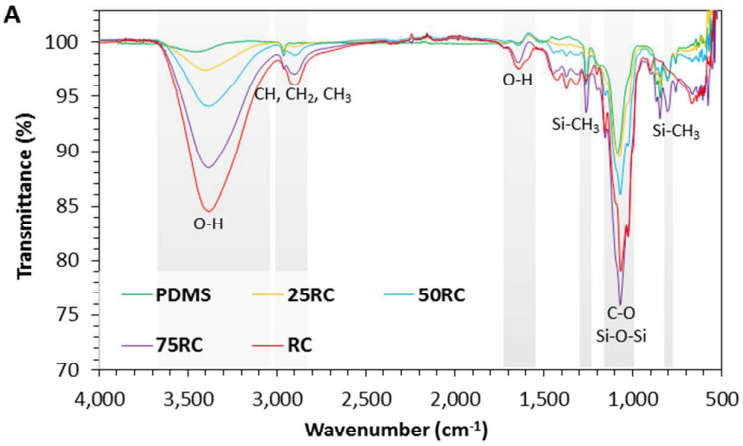

B

Membrane	Atomic composition (%)		
	C	O	Si
PDMS6	45.3	28.5	26.2
25RC	56.4	24.8	18.2
50RC	56.9	32.5	10.6
75RC	56.3	33.1	7.9
RC	60.7	39.3	0

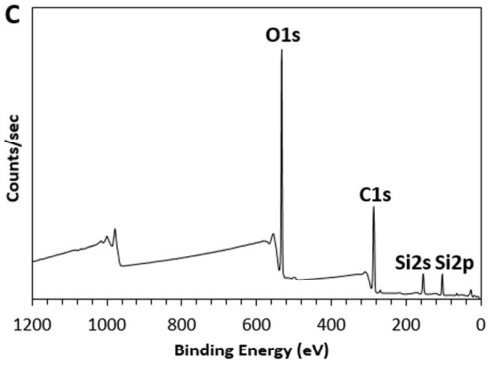

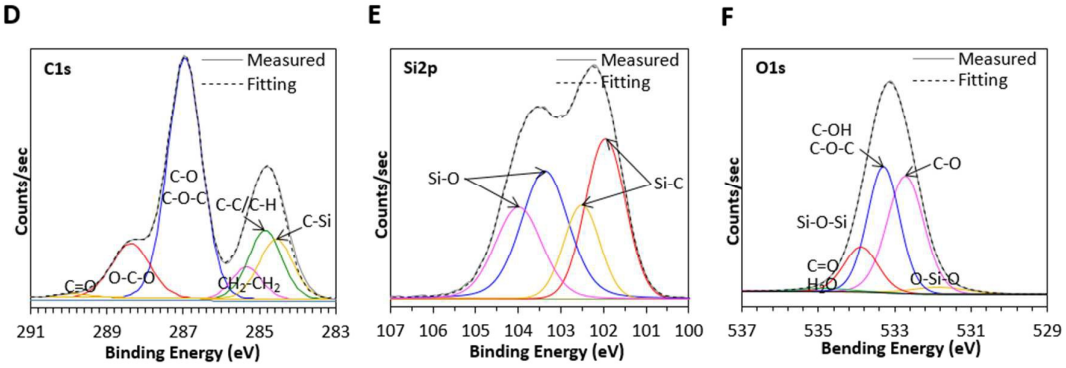

Figure 3 Membrane chemistry. **A.** ATR-IR spectra and **B.** XPS atomic composition of different composition of the blend membranes. **C.** XPS survey of the 50RC membrane revealing the curve-fitting in the **D.** C1s, **E.** Si2p, and **F.** O1s region.

View Article Online
DOI: 10.1039/C8TA02697A

asymmetric Si-O-Si stretching evidenced between 1,055-1,090 cm^{-1}. For the polymer blends the spectra show the signature of cellulose bands between 3,050-3,700 cm^{-1} and 1,060 cm^{-1} attributed to the strong O-H and C-O bonds, respectively. With the increasing cellulose content in the membranes, the intensity of the cellulose characteristics band was higher accompanied by the simultaneous decreasing intensity of the silicon-related peaks. This was also followed by the slightly higher intensity of the alkane related peaks around 2,900 cm^{-1} attributed to CH, CH_2 and CH_3 as well as O-H bending vibration near 1,660 cm^{-1} raised from the cellulose backbone. Further elucidation of the membrane chemistry was carried out by measuring the atomic composition of all membranes using XPS. The results presented in Figure 3B clearly demonstrate the proportional decrease of silicon content in the membranes corresponding to their compositions. It can also be seen that the pure RC membrane did not contain any silicon, suggesting that the performed hydrolysis method has allowed the complete transformation of TMSC back to cellulose. Accordingly, we anticipated that the silicon-related peaks appearing in the blend membranes were associated only with PDMS. Bonding configuration was performed on the 50RC membrane. Figure 3C displays the XPS survey spectra, while Figure 3D, 3E and 3F present the high-resolution curve fitting in the C1s, Si2p and O1s region respectively using the Lorentzian-Gaussian function. The high-resolution spectra reveal the presence of PDMS characteristic bonds consisting of C-Si and CH_2-CH_2 peak at 284.6 and 285.4 eV respectively and all the silicon related peaks in Si2p and O1s region. The intense peaks specifically attributed to cellulose consist of the C-O related peaks at around 287 and 288.5 eV located in the C1s region, as well as near 534 and 533 eV in the O1s region.

The introduction of cellulose in the membranes also significantly affected the final surface properties. It is well-accepted that membranes with a strong hydrophilic character tend to permeate polar solvents better than those with low polarity and vice versa. The membrane wettability is also responsible for the swelling phenomenon, which could severely affect the membrane performance. The data presented in Figure 4 shows the decreasing water contact angle from around 80° for the pure PDMS, which is similar to the values reported in the literature[26], to below 30° for the pure cellulose (RC). When cellulose concentrations increased in the 25RC and 50RC membranes, the surfaces were still very

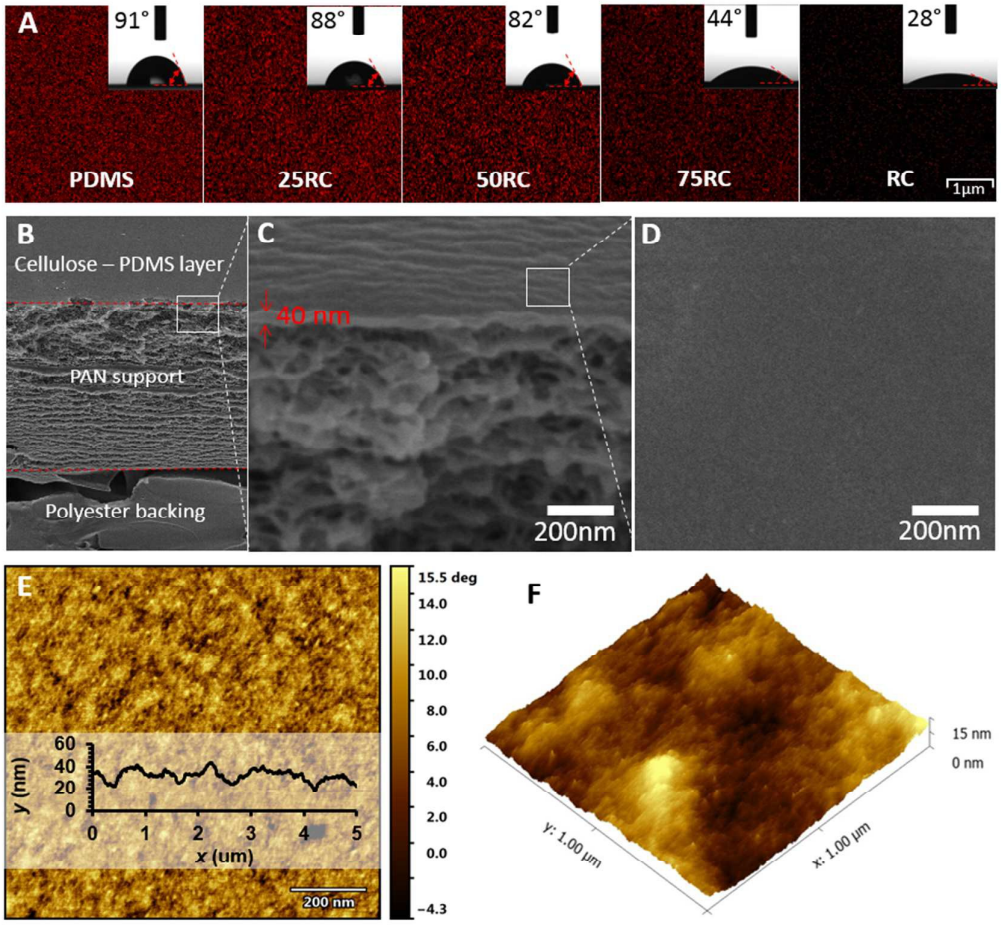

Figure 4 Membrane surface properties. **A.** EDX silicon map and the corresponding static water contact angle of different composition of the blend membranes, **B-C.** cross-sectional and **D.** surface SEM images, **E.** AFM contrast-phase and **F.** topographic image of the 50RC membrane.

View Article Online
DOI: 10.1039/C8TA02697A

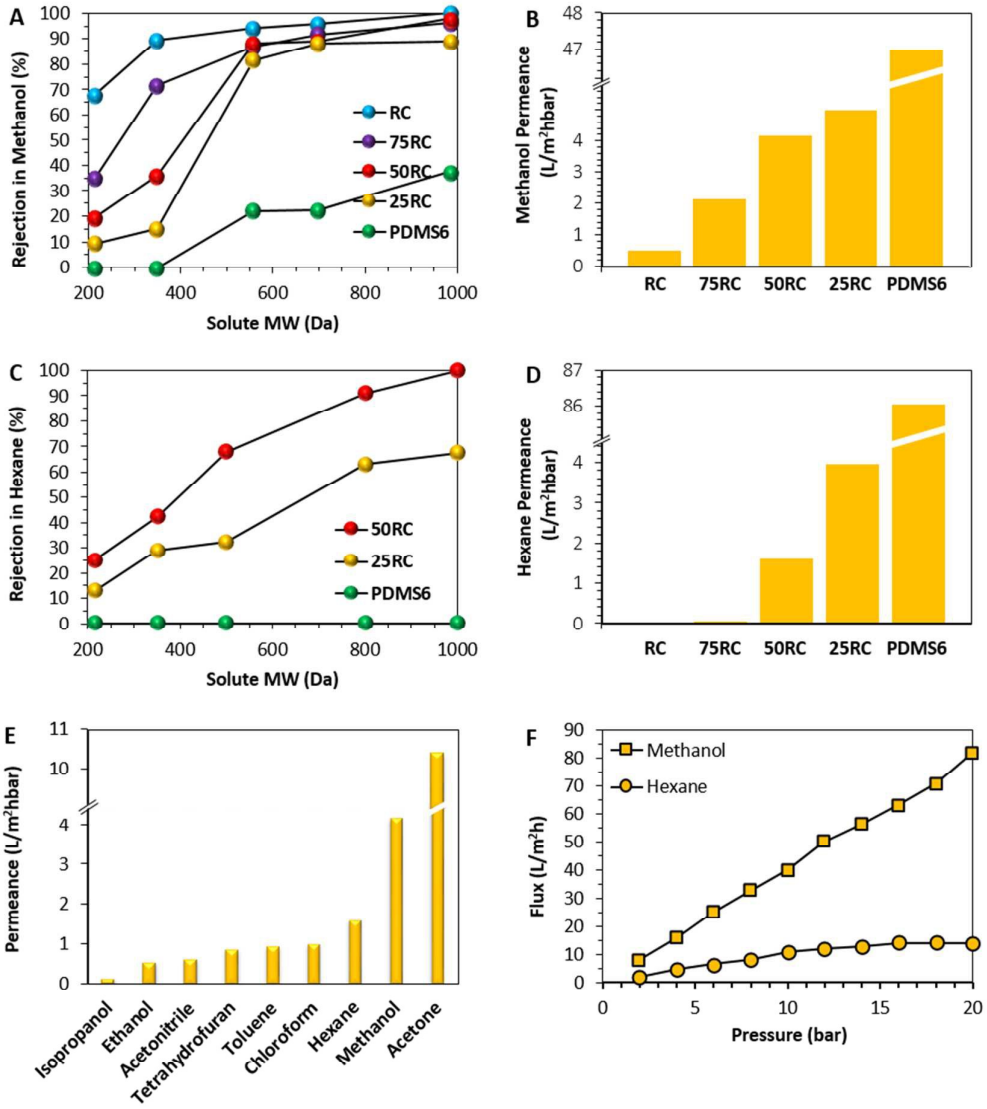

Figure 5 OSN performance. **A.** Rejection and **B.** flux in methanol, **C.** rejection and **D.** flux in hexane, **E.** pure solvent permeances, and **F.** the effects of compaction during methanol and hexane filtration on the 50RC membrane. Feed pressure in experiment A-E: 8 bar.

hydrophobic with the water contact angle slightly below that of PDMS. A significantly lower contact angles of about 40° was observed for the 75RC membrane. According to Figure 4B-D, the 50RC membrane displayed a highly smooth layer without any observable defects. The active layer with an approximate thickness of 40 nm adhered very well to the porous support. The membrane also demonstrated a good uniformity as depicted by the AFM images (Figure 4E-F).

3.3 OSN Performance

In this study, membranes consisting of different ratios of cellulose and PDMS were evaluated in the filtration of different organic solvents. As listed in Table 1, the total polymer concentration in the coating solution was fixed to be 2 wt%, except for the case of pure PDMS membranes where a minimum solution concentration of 6 wt% was required to acquire defect-free membranes. The quality of the PDMS membranes was first confirmed by studying the oxygen and nitrogen permeation. The intrinsic O_2/N_2 selectivity of pure PDMS membranes, which is around 2.1[27-30], was achieved using 6 wt% solution concentration (PDMS6), whereas the selectivities of the PDMS2 and PDMS4 membranes were lower, indicating the presence of defects. Benefiting from the cellulose/TMSC properties, the cellulose-PDMS blend membranes can be fabricated with only 2 wt% solution concentration leading to thin membranes with high solvent fluxes.

Figure 5 reveals that the pure regenerated cellulose and the pure silicone rubber membrane show very different filtration performance as expected. The RC membrane

View Article Online
DOI: 10.1039/C8TA02697A

exhibited a size selectivity with a molecular weight cut-off (MWCO) of around 300 Da combined with a methanol permeance of about 0.5 L/m^{2}hbar (Figure 5A and B). In contrast, the PDMS6 membrane showed a very poor selectivity combined with a very high permeance. In the permeation of hexane (Figure 5C and 5D), the RC membrane did not display any permeance as expected from its strong hydrophilic character (see Figure 4A), while the PDMS6 membrane completely lost its selectivity due to excessive swelling.

Interestingly, a favorable combination between cellulose selectivity and PDMS flexibility was achieved using the blend membranes. The introduction of a small portion of TMSC in the 25RC membrane substantially improved the membrane sieving properties both in methanol and hexane filtration. By using neutral dyes in methanol, the membrane demonstrated more than 80% rejection of bromopyrogallol red (615 Da) and around 90% of tetrabromophenol blue (986 Da), suggesting an approximately 1,000 Da MWCO. Similar rejections were also obtained using the different neutral markers in hexane. Permeances as high as 4 and 5 L/m^{2}hbar of pure methanol and pure hexane respectively were measured using this membrane. Increasing the cellulose percentage to 50% in the 50RC membrane further enhanced the rejection especially toward the solutes with molecular weight of 558 Da and higher, resulting in an estimated MWCO of about 750 Da in both solvents. The methanol permeance of this membrane was about 4.2 L/m^{2}hbar for pure methanol and 1.6 L/m^{2}hbar for pure hexane. With the domination of cellulose in the 75RC membrane, the MWCO was estimated to be about 650 Da in methanol with around 2 L/m^{2}hbar permeance. However, the hexane permeance dropped significantly attributed to the dominant contribution of cellulose in the membrane wettability as indicated by its low water contact angle (Figure 4A). On the one hand, the incorporation of cellulose into the PDMS matrix reduced the PDMS chain flexibility resulting in a better molecular sieving. On the other hand, the presence of PDMS in the cellulose network interrupted the densely packed cellulose structure, promoting higher solvent fluxes especially in the case of non-polar solvents (e.g. hexane). The 50/50 blend (50RC membrane) is a favorable trade-off, showing good fluxes and selectivities in polar and non-polar solvents.

Encouraged by the good filtration results with methanol and hexane, we tested the 50RC membrane with seven more solvents. Methanol and hexane, which represent the most polar and non-polar solvent among the list, gave reasonably high permeances, signifying that the membrane performances were barely controlled by the solvent polarity. This is because the membrane contained both highly polar and highly non-polar polymer chains, allowing the easy passage of the solvent with any polarity. According to Figure 5E, the highest permeance of 10.5 L/m^{2}hbar was achieved using acetone, the lowest permeance of 0.1 L/m^{2}hbar was obtained using isopropanol, which is the most viscous solvent tested in the study, while the rest of the solvents showed acceptable permeance values between 0.5-1 L/m^{2}hbar. It is well known, that increasing solvent viscosity reduces the solvent permeance[31-35]. However, acetone had the highest permeance in our experiment, but it did not have the lowest viscosity, indicating that other parameters such as solubility[32, 33], solvent sizes[33] as well as surface energy between the membrane and solvent [32, 33, 35, 36] might affect the permeation rate. Considering that the rejection properties are similar for the filtration of methanol and hexane (Figure 5A and 5C), we anticipated similar rejections using other solvents, including acetone.

The effect of the feed pressure on the flux of methanol and hexane through the 50RC membrane was tested between 2 and 20 bar (Figure 5F). No compaction effect could be observed in the case of methanol filtration in the applied pressure range; a slight flux decline took place in the case of hexane at a pressure above 12 bar. Compaction is usually caused by the support layer; the small effects observed in this study can be attributed to the good structural feature of the PAN layer with the absence of macrovoids (see Figure 4B and 4C). However, the different responses given in both filtrations also indicated the minor contribution of the top layer structure on the compaction. Overall, the good OSN performance obtained by the blend membranes is based on the successful combination of the cellulose selectivity and PDMS permeability. The simple membrane fabrication and the fact that the membranes can be applied for polar and non-polar solvents could broaden the range of OSN applications.

3.4 Pervaporation Performance

Motivated by the intriguing performance of the PDMS/cellulose blend membranes for organic solvent nanofiltration we tested these membranes for the separation of water-rich ethanol-water streams by pervaporation. In pervaporation the liquid feed stream contacts the membrane and the permeate is transported through the membrane, withdrawn as vapor and then condensed.

Industrially, classic distillation separates water-rich ethanol-water streams, and pressure-swing/azeotropic-extractive units are applied for ethanol-rich azeotropic mixtures (requiring massive use of energy/solvents[37-39]). In pervaporation, a membrane enhances the evaporation of a target mixture-compound and ethanol can be separated from water consuming a fraction of the energy required for distillation; ideally, for a membrane with infinite selectivity, the energy could be limited to the heat of evaporation of the ethanol (or water) of the feed. Hydrophobic pervaporation of water-rich streams may be a breakthrough technology for bioethanol upgrading[40]; this separation is difficult since water has a diffusion advantage, limiting ethanol enrichment. Many studies were already reported in the literature about ethanol selective membranes for pervaporation; mainly, PDMS-based membranes were studied in the supported/unsupported[41-44], blended[45-47], or in a mixed-matrix configuration[48-52].

View Article Online
DOI: 10.1039/C8TA02697A

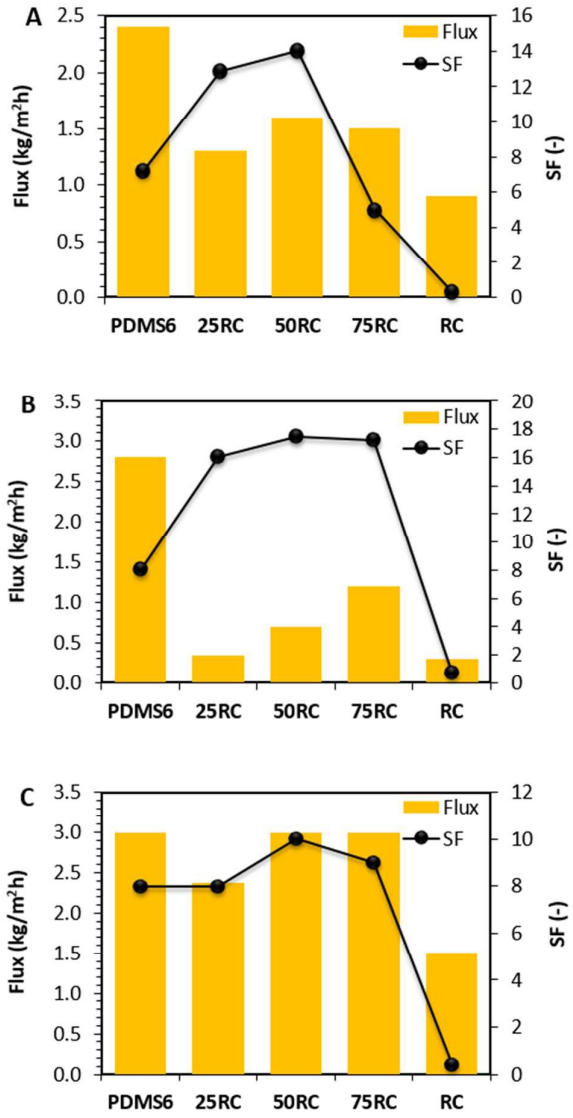

Figure 6 Pervaporation performance of different composition of the blend membranes. **A.** 5 wt% ethanol/water feed at 24°C and 10 wt% ethanol/water feed at **B.** 24°C and **C.** 60°C.

Two different feed mixtures containing 5 wt% and 10 wt% ethanol, which mimic the composition of the fermentation broths[53], were investigated at different operating temperatures. Different composition of cellulose-PDMS membranes were first evaluated in the pervaporation of aqueous feed containing 5 wt% ethanol at ambient temperature. Under these conditions the pure PDMS membrane (PDMS6) showed a separation factor of 7.2, similar to the values reported in the literature[54, 55], with a flux of 2.4 kg/m^{2}h (Figure 6A). On the other hand, the pure RC membrane expectedly gave a reverse (water selective) separation factor of 0.3 due to its strong hydrophilic property. Interestingly, blending PDMS with RC allows increasing the ability of the membrane to pervaporate ethanol. This result seems to be counterintuitive since PDMS is hydrophobic while RC is hydrophilic, and we speculate the presence of the RC in the matrix forces water through slower diffusion paths (as schematically illustrated in Figure S4). In comparison with pure PDMS, water diffusivity is reduced and ethanol/water separation factor enhanced. Similar behavior was already reported by Lue *et al.*[50] who showed how filling PDMS with a commercial zeolite decreased ethanol/water solubility selectivity and increased ethanol/water permeability selectivity. With the presence of small percentage of cellulose in the 25RC membranes, the separation factor significantly rose to 12.9, accompanied by the flux decrease to 1.3 kg/m^{2}h. A 50:50 ratio between the polymer components in the 50RC membrane led to even more interesting results where a separation factor of 14 was achieved, which doubled the separation factor of the pure PDMS, with just slightly compromising the PDMS flux to 1.6 kg/m^{2}h. As a comparison, using a similar feed concentration at 30°C, the commercial Pervap 4060 (Sulzer ChemTech, Switzerland) and Pervatech PDMS (Pervatech BV, The Netherlands) have a flux of 0.6 and 1kg/m^{2}h with separation factors of 8.4 and 5.2, respectively[56].

Figure 6B and 6C demonstrate the performance of the membranes using 10 wt% ethanol/water feed. With higher ethanol content in the feed running at 24°C, the performance of the pure membranes was similar to the one with 5 wt% ethanol/water, while all the blend membranes presented remarkably higher separation factors with lower fluxes. The 50RC membrane exhibited the highest separation factor of 17.5, which is more than twice the separation factor of the pure PDMS membrane. Operating the experiment at higher temperature of 60°C expectedly led to higher fluxes and lower separation factors as presented in Figure 6C. The higher fluxes in the experiments with higher temperature can be attributed to the higher diffusion rate of the solvent molecules as well as the enhanced driving force across the membrane, whereas the separation factor decreases mainly because of the lower solubility selectivity. Remarkably, in this experiment the 50RC membrane displayed a similar flux as the PDMS6 membrane, while presenting a higher separation factor of 10. This emphasizes that the introduction of cellulose into the PDMS matrix facilitates the selective ethanol transport while maintaining the exceptionally high flux of PDMS. More interestingly, the superiority of our blend membrane over the commercial membranes is again displayed using similar test conditions. The performance obtained with a 10% ethanol feed confirms again that the PDMS/cellulose blend membrane is competitive with commercial membranes. Pervaporation of 10 wt% ethanol at 50°C using the Pervap 4060 gives a 1.9 kg/m^{2}h flux and 7 SF whereas the Pervatech PDMS shows a 3.3 kg/m^{2}h flux with a lower SF of 6[57].

Conclusions

Homogeneous blends of polydimethylsiloxane with cellulose have been introduced for the first time. The blending of these very different polymers was possible via a "Trojan-horse" method. The cellulose was first transformed into an

View Article Online
DOI: 10.1039/C8TA02697A

amorphous hydrocarbon soluble polymer by functionalization with trimethylsilyl groups. The trimethylsilyl cellulose could then be blended in solution with PDMS. Composite membranes were manufactured by solution coating of a porous UF membrane. Finally the cellulose was regenerated by treatment with hydrochloric acid vapor leading to very thin unique PDMS/cellulose blend layers acting as selective membranes for organic solvent nanofiltration and pervaporation. The interplay between the two polymers – one hydrophilic and rigid, the other one hydrophobic and flexible – led to membranes with significantly enhanced separation performance when compared with the pure polymer membranes. In the case of organic solvent nanofiltration the cellulose present in the interpenetrating PDMS/cellulose network reduced the swelling of the PDMS by the organic solvent and increased the membranes selectivity without large flux reduction. Due to the nature of the blend the membranes can be used with polar and non-polar solvents. In the case of pervaporation of water/ethanol mixtures the addition of the water selective cellulose to PDMS surprisingly resulted in blend membranes with significantly enhanced ethanol separation ability. The presence of the cellulose in the matrix forces water through slower diffusion paths and in comparison with pure PDMS, water diffusivity is reduced and ethanol/water separation factor enhanced.

Conflicts of interest

There are no conflicts to declare.

Acknowledgements

This research was carried out under funding from King Abdullah University of Science and Technology (KAUST, Saudi Arabia) Center of Advanced Membranes and Porous Materials. The authors thank Ohoud Al-Harbi, Nini Wei, Nemar Al-Wehbi and Wandi Wahyudi for their help with SEM, EDX and XPS analysis.

References

1. Solvents - Study: Market, Analysis, Trends | Ceresana, http://www.ceresana.com/en/market-studies/chemicals/solvents/, (accessed 8 November, (accessed: November 2017)).
2. D. S. Sholl and R. P. Lively, *Nature*, 2016, **532**, 435-437.
3. P. Vandezande, L. E. M. Gevers and I. F. J. Vankelecom, *Chem. Soc. Rev.*, 2008, **37**, 365-405.
4. G. Székely, J. Bandarra, W. Heggie, B. Sellergren and F. C. Ferreira, *J. Membr. Sci.*, 2011, **381**, 21-33.
5. D. Ormerod, B. Sledsens, G. Vercammen, D. Van Gool, T. Linsen, A. Buekenhoudt and B. Bongers, *Sep. Purif. Technol.*, 2013, **115**, 158-162.
6. G. Cederløf and E. R. Geus, US Patent 7351873, 2008.
7. A. P. B. Ribeiro, J. M. de Moura, L. A. Gonçalves, J. C. C. Petrus and L. A. Viotto, *J. Membr. Sci.*, 2006, **282**, 328-336.
8. U. Razdan, S. Joshi and V. Shah, *J. Curr. Sci.*, 2003, **85**, 761-771.
9. S. Sorribas, P. Gorgojo, C. Téllez, J. Coronas and A. G. Livingston, *J. Am. Chem. Soc*, 2013, **135**, 15201-15208.
10. Y. K. Ong, G. M. Shi, N. L. Le, Y. P. Tang, J. Zuo, S. P. Nunes and T. S. Chung, *Prog. Polym. Sci.*, 2016, **57**, 1-31.
11. L. Ulljltmb·, L. Le and C. Lorraine, in *Effective industrial membrane processes: benefits and opportunities*, ed. M. K. Turner, Springer Science & Business Media, 1991, pp. 281-293.
12. H. L. Fleming and C. S. Slater, in *W.S.W. Ho, K.K. Sirkar (Eds.), Membrane Handbook*, Van Nostrand Reinhold, New York, 1992, ch. 10, p. 150.
13. N. Bosq, N. Guigo, J. Persello and N. Sbirrazzuoli, *Phys. Chem. Chem. Phys.*, 2014, **16**, 7830-7840.
14. P. Klonos, G. Dapei, I. Y. Sulym, S. Zidropoulos, D. Sternik, A. Deryło-Marczewska, M. V. Borysenko, V. M. Gun'ko, A. Kyritsis and P. Pissis, *Eur. Polym. J.*, 2016, **74**, 64-80.
15. H. B. Park, C. K. Kim and Y. M. Lee, *J. Membr. Sci.*, 2002, **204**, 257-269.
16. X. Zhao, Y. Su, Y. Li, R. Zhang, J. Zhao and Z. Jiang, *J. Membr. Sci.*, 2014, **450**, 111-123.
17. S. R. Reijerkerk, M. H. Knoef, K. Nijmeijer and M. Wessling, *J. Membr. Sci.*, 2010, **352**, 126-135.
18. T. Miyata, T. Takagi, T. Kadota and T. Uragami, *Macromol. Chem. Phys.*, 1995, **196**, 1211-1220.
19. T. Ohshima, Y. Kogami, T. Miyata and T. Uragami, *J. Membr. Sci.*, 2005, **260**, 156-163.
20. W. Liu, Y. Li, X. Meng, G. Liu, S. Hu, F. Pan, H. Wu, Z. Jiang, B. Wang, Z. Li and X. Cao, *J. Mater. Chem. A*, 2013, **1**, 3713-3713.
21. P. Garg, R. P. Singh and V. Choudhary, *Sep. Purif. Technol.*, 2011, **76**, 407-418.
22. T. Puspasari, F. H. Akhtar, W. Ogieglo, O. Alharbi and K.-V. Peinemann, *J. Mater. Chem. A*, 2018, DOI: 10.1039/C8TA00350E.
23. T. Puspasari and K.-V. Peinemann, *J. Water Process Eng.*, 2016, **13**, 176-182.
24. T. Puspasari, N. Pradeep and K.-V. Peinemann, *J. Membr. Sci.*, 2015, **491**, 132-137.
25. T. Puspasari, H. Yu and K. -V. Peinemann, *ChemSusChem*, 2016, **9**, 2908-2911.
26. M. Razali, C. Didaskalou, J. F. Kim, M. Babaei, E. Drioli, Y. M. Lee and G. Szekely, *ACS Appl. Mater. Interfaces*, 2017, **9**, 11279-11289.
27. K. Kammermeyer, *Industrial & Engineering Chemistry*, 1957, **49**, 1685-1686.
28. W. Robb, *Ann. N. Y. Acad. Sci.*, 1968, **146**, 119-137.
29. I. De Bo, H. Van Langenhove, P. Pruuost, J. De Neve, J. Pieters, I. F. J. Vankelecom and E. Dick, *J. Membr. Sci.*, 2003, **215**, 303-319.
30. S. Shishatskiy, C. Nistor, M. Popa, S. P. Nunes and K. -V. Peinemann, *Adv. Eng. Mater.*, 2006, **8**, 390-397.
31. S. Karan, Z. Jiang and A. G. Livingston, *Science*, 2015, **348**, 1347-1351.
32. J. Robinson, E. Tarleton, C. Millington and A. Nijmeijer, *J. Membr. Sci.*, 2004, **230**, 29-37.
33. D. Bhanushali, S. Kloos, C. Kurth and D. Bhattacharyya, *J. Membr. Sci.*, 2001, **189**, 1-21.
34. P. Silva, S. Han and A. G. Livingston, *J. Membr. Sci.*, 2005, **262**, 49-59.
35. D. R. Machado, D. Hasson and R. Semiat, *J. Membr. Sci.*, 1999, **163**, 93-102.
36. H. Zwijnenberg, A. M. Krosse, K. Ebert, K.-V. Peinemann and F. Cuperus, *J. Am. Oil Chem.' Soc.*, 1999, **76**, 83-87.
37. G. Genduso, A. Amelio, E. Colombini, P. Luis, J. Degrève and B. Van der Bruggen, *Chem. Eng. Res. Des.*, 2016, **109**, 127-140.
38. B. K. Dutta and S. K. Sikdar, *AIChE journal*, 1991, **37**, 581-588.

View Article Online
DOI: 10.1039/C8TA02697A

39. G. Genduso, A. Amelio, P. Luis, Van der B. Bruggen and S. Vreysen, *AIChE Journal*, 2014, **60**, 2584-2595.
40. B. Van der Bruggen and P. Luis, *Curr. Opin. Chem. Eng.*, 2014, **4**, 47-53.
41. I. Blume, J. Wijmans and R. Baker, *J. Membr. Sci.*, 1990, **49**, 253-286.
42. C.-L. Chang and M.-S. Chang, *J. Membr. Sci.*, 2004, **238**, 117-122.
43. P. V. Naik, R. Bernstein and I. F. J. Vankelecom, *J. Appl. Polym. Sci.*, 2016, **133**, 1-12.
44. L. M. Vane, *J. Chem. Technol. Biotechnol.*, 2005, **80**, 603-629.
45. I. Ahmed, N. F. C. Pa, M. G. M. Nawawi and W. A. W. A. Rahman, *J. Appl. Polym. Sci.*, 2011, **122**, 2666-2679.
46. L. Liang and E. Ruckenstein, *J. Membr. Sci.*, 1996, **114**, 227-234.
47. S. Takegami, H. Yamada and S. Tsujii, *J. Membr. Sci.*,1992, **75**, 93-105.
48. M.-D. Jia, K.-V. Pleinemann and R.-D. Behling, *J. Membr. Sci.*,1992, **73**, 119-128.
49. Q. Li, L. Cheng, J. Shen, J. Shi, G. Chen, J. Zhao, J. Duan, G. Liu and W. Jin, *Sep. Purif. Technol.*, 2017, **178**, 105-112.
50. S. J. Lue, C.-F. Chien and K. Mahesh, *J. Membr. Sci.*, 2011, **384**, 17-26.
51. N. Wang, G. Shi, J. Gao, J. Li, L. Wang, H. Guo, G. Zhang and S. Ji, *Sep. Purif. Technol.*, 2015, **153**, 146-155.
52. H. Yin, C. Y. Lau, M. Rozowski, C. Howard, Y. Xu, T. Lai, M. E. Dose, R. P. Lively and M. L. Lind, *J. Membr. Sci.*, 2017, **529**, 286-292.
53. H.-J. Huang, S. Ramaswamy, U. W. Tschirner and B. V. Ramarao, *Sep. Purif. Technol.*, 2008, **62**, 1-21.
54. P. V. Naik, P. L. H. Verlooy, S. Smet, J. A. Martens and I. F. J. Vankelecom, *RSC Adv.*, 2016, **6**, 78648-78651.
55. P. V. Naik, L. H. Wee, M. Meledina, S. Turner, Y. Li, G. Van Tendeloo, J. A. Martens and I. F. J. Vankelecom, *J. Mater. Chem. A*, 2016, **4**, 12790-12798.
56. S. Chovau, S. Gaykawad, A. J. Straathof and B. Van der Bruggen, *Bioresour. Technol.*, 2011, **102**, 1669-1674.
57. S. Claes, P. Vandezande, S. Mullens, R. Leysen, K. De Sitter, A. Andersson, F. H. Maurer, H. Van den Rul, R. Peeters and M. Van Bael, *J. Membr. Sci.*, 2010, **351**, 160-167.